

Actin Cross-Linking and Inhibition of the Actomyosin Motor[†]

Eldar Kim,^{‡,§} Elena Bobkova,[‡] György Hegyi,^{||} Andras Muhrad,^{‡,⊥} and Emil Reisler^{*,‡}

Department of Chemistry and Biochemistry and Molecular Biology Institute, University of California, Los Angeles, California 90095, and Department of Biochemistry, Eötvös Lorand University, H-1088 Budapest, Hungary

Received July 2, 2001; Revised Manuscript Received October 1, 2001

ABSTRACT: Intrastrand cross-linking of actin filaments by ANP, *N*-(4-azido-2-nitrophenyl) putrescine, between Gln-41 in subdomain 2 and Cys-374 at the C-terminus, was shown to inhibit force generation with myosin in the in vitro motility assays [Kim et al. (1998) *Biochemistry* 37, 17801–17809]. To clarify the immobilization of which of these two sites inhibits the actomyosin motor, the properties of actins with partially overlapping cross-linked sites were examined. pPDM (*N,N'*-*p*-phenylenedimaleimide) and ABP [*N*-(4-azidobenzoyl) putrescine] were used to obtain actin filaments cross-linked (~50%) between Cys-374 and Lys-191 (interstrand) and Gln-41 and Lys-113 (intrastrand), respectively. ANP, ABP, and pPDM cross-linked filaments showed similar inhibition of their sliding speeds and force generation with myosin (~25%) in the in vitro motility assays. In analogy to ANP cross-linking of actin, pPDM and ABP cross-linkings did not change the strong S1 binding to actin and the V_{\max} and K_m parameters of actomyosin ATPase. The similar effects of these three cross-linkings reveal the tight coupling between structural elements of the subdomain 2/subdomain 1 interface and show the importance of its dynamic flexibility to force generation with myosin. The possibility that actin cross-linkings inhibit rate-limiting steps in motion and force generation during myosin cross-bridge cycle was tested in stopped-flow experiments. Measurements of the rates of mantADP release from actoS1 and ATP-induced dissociation of actoS1 did not reveal any differences between un-cross-linked and ANP cross-linked actin in these complexes. These findings are discussed in terms of the uncoupling between force generation and other aspects of actomyosin interactions due to a constrained dynamic flexibility of the subdomain 2/subdomain 1 interface in cross-linked actin filaments.

Actin dynamics play a major role in many cellular processes including cell motility, endocytosis, exocytosis, cell division, and others. These processes depend on the reorganization of actin assemblies, and, in some cases, they may involve significant changes in the actin filament structure (1–3). The well-documented transitions in the actin filament twist induced by cofilin (1, 4, 5) have been shown to occur also, albeit at different frequency, in actin alone (5). This observation is consistent with and supports a large body of work of the Egelman group showing the equilibration of actin among different conformational states, depending on the nucleotides, divalent cations, and proteins bound to it (6–8). These and other studies implicated the subdomain 2 and C-terminal regions (in subdomain 1) as the main dynamic elements that are involved in such structural transitions.

The potential significance of F-actin dynamics, and in particular at the subdomain 2/subdomain 1 interface, is obvious in the context of cytoskeletal actin remodeling, but

is less clear in the process of force generation by actomyosin. Experimental tests of the role of actin dynamics in that process are not free of ambiguities. Even in the case of specific modifications of Cys-374 on actin, with pyrene maleimide and IEDANS,¹ the resulting changes in actomyosin interactions may be due to either direct or indirect effects on myosin binding, or perhaps changes in actin dynamics. Cross-linkings and proteolytic cleavage reactions offer a more direct route to altering protein dynamics, but their effects may also be open to alternative interpretations. Such has been the case with the previously reported inhibition of the in vitro motility of actin filaments due to intramolecular carbodiimide cross-linking of actin protomers (9) and with the subtilisin cleavage of the DNaseI loop, between Met-47 and Gly-48 (10). In the former treatment, the loss of motile function in copolymers of cross-linked and un-cross-linked actin resulted probably from a combination of at least two factors: the inability of cross-linked actin to activate the myosin ATPase, and the possible requirement for two adjacent unmodified actin protomers for such an activation. In the latter case, both the actomyosin ATPase (K_m value) and the binding of myosin

[†] This work was supported by U.S. Public Health Service Grant AR 22031 and by National Science Foundation Grant MCB 9904599.

* Address correspondence to this author. Phone: (310) 825-2668. Fax: (310) 206-7286. E-mail: reisler@mbi.ucla.edu.

[‡] University of California, Los Angeles.

[§] Present address: Department of Molecular Biology, Massachusetts General Hospital, Boston, MA 02114.

^{||} Eötvös Lorand University.

[⊥] Permanent address: Department of Oral Biology, Hebrew University Hadassah School of Dental Medicine, Jerusalem 91120, Israel.

¹ Abbreviations: ANP, *N*-(4-azido-2-nitrophenyl) putrescine; ABP, *N*-(4-azidobenzoyl) putrescine; pPDM, *N,N'*-*p*-phenylenedimaleimide; DTT, dithiothreitol; IEDANS, 5-(2-((iodoacetyl)amino)ethyl)aminonaphthalene-1-sulfonate; SDS-PAGE, sodium dodecyl sulfate-polyacrylamide gel electrophoresis; PIPES, piperazine-*N,N'*-bis(2-ethanesulfonic acid); S1, myosin subfragment 1; HMM, heavy meromyosin.

were shown to be changed at least 10-fold by the actin cleavage (11), making a direct link between changes in filament flexibility and dynamics and the inhibition of motility less unambiguous.

The more recent specific cross-linking of actin filament by *N*-(4-azido-2-nitrophenyl) putrescine (ANP), bridging between Gln-41 and Cys-374 on adjacent protomers within the same strand (12, 13), appears to provide more detailed information on the link between actin's motility and its structure and dynamics. The labeling of Gln-41 on skeletal α -actin by ANP without the cross-linking (13), and the zero-length (transglutaminase-mediated) intramolecular cross-linking of Gln-41 to Lys-50 did not alter actin's *in vitro* motility (14). However, the motion of actin over myosin was strongly inhibited by interprotomer ANP cross-linking of Gln-41 to Cys-374 on F-actin (13). These results suggest a link between the conformational freedom of the subdomain 2/subdomain 1 interprotomer interface (which is constrained by Gln-41–Cys-374 cross-linking) and the mechanical function of the actomyosin motor system. Interestingly, other parameters that describe actomyosin interactions, including binding constants and the K_m and V_{max} values of the ATPase activity, were affected much less by the cross-linking than the *in vitro* motility of actin.

Subsequent work provided evidence that the interprotomer Gln-41–Cys-374 cross-linking induces only minimal changes in F-actin structure, as represented by the Holmes et al. model (15). This conclusion is based on electron microscopy image reconstruction analysis of wild-type and disulfide cross-linked and un-cross-linked yeast mutant actin filaments, in which Gln-41 was substituted with a cysteine residue (16). The facile formation of interprotomer disulfide bonds between Cys-41 and Cys-374 in such yeast mutant F-actin is another indication of the dynamic nature of the subdomain 2/subdomain 1 interface in actin filaments; the distance between the C- α atoms of these residues is ~ 11 Å in the Holmes et al. model of F-actin structure (15).

Although the results of the above studies suggest that arresting dynamic rearrangements of subdomain 2 vs subdomain 1 in actin filaments inhibits their *in vitro* motility, it is not obvious whether the dynamic freedom of both regions is equally important to actin's function and, if not, the immobilization of which element inhibits the motility of actin. Our goal in this study has been to refine the dynamics–function mapping of the subdomain 2/subdomain 1 interface in F-actin and to establish a direct link between a specific structural element of actin and its motility. To this end, we took advantage of three cross-linking reagents, ANP, *N*-(4-azidobenzoyl) putrescine (ABP), and *p*-phenylenedimaleimide (pPDM), which form cross-links on F-actin between Gln-41 and Cys-374 (12), Gln-41 and Lys-113 (17), and Cys-374 and Lys-191 (18, 19), respectively. These reagents provide the tools for immobilizing the Gln-41 and Cys-374 regions in tandem and separately. Functional analysis of actin filaments cross-linked (approximately 50%) by these reagents revealed similar inhibition of their force and motion-generating function with myosin. Our results show a tight coupling between the structural elements of the subdomain 2/subdomain 1 interface and reveal that conformational freedom must be retained at this interface for actin to generate motion and force with myosin.

MATERIALS AND METHODS

Reagents. Synthesis of ANP [*N*-(4-azido-2-nitrophenyl) putrescine] and ABP [*N*-(4-azidobenzoyl) putrescine] was described in prior publications (12, 17). pPDM (*N,N'*-*p*-phenylenedimaleimide), ATP, ADP, and phalloidin were obtained from Sigma Chemical Co. (St. Louis, MO). Rhodamine phalloidin was purchased from Molecular Probes (Eugene, OR). Ca^{2+} -independent bacterial transglutaminase was a generous gift from Dr. K. Seguro (Ajimoto Co. Inc., Kawasaki, Japan).

Proteins. Rabbit skeletal α -actin and myosin were prepared according to the methods of Spudich and Watt (20) and Godfrey and Harrington (21), respectively. Myosin subfragment 1 (S1) and heavy meromyosin (HMM) were prepared following the procedures of Weeds and Pope (22) and Margossian and Lowey (23), respectively.

Actin Labeling and Cross-Linking. For ANP and ABP labeling, G-actin (2.0 mg/mL) was incubated with these reagents (at 8 M excess) and the transglutaminase (0.5 unit/mL) in G-actin buffer (4.0 mM Tris-HCl, pH 7.6, 0.4 mM ATP, and 0.2 mM CaCl_2) in the dark, for 2 h at room temperature. This labeling procedure yields between 0.7 and 0.95 mol of ANP incorporated into G-actin (13), and somewhat less ABP. To obtain various degrees of actin cross-linking, we copolymerized ANP and ABP G-actin with different amounts of unlabeled G-actin by 2.0 mM MgCl_2 . The resulting F-actin was pelleted by centrifugation at 40 000 rpm for 2 h in a Beckman 55.2 Ti rotor. The F-actin pellet was homogenized in F-actin buffer (4.0 mM Tris-HCl, pH 7.6, 0.2 mM ATP, and 2.0 mM MgCl_2) and then incubated for 1–2 h on ice in the dark. The photo-cross-linking of F-actin was carried out as described earlier (12, 13). β -Mercaptoethanol was added to quench the unreacted arylazido compound.

The pPDM labeling and cross-linking of F-actin were done according to Knight and Offer (18). To determine the percentage of actin cross-linked by ANP, ABP, and pPDM, aliquots of the cross-linked actin were denatured and examined on SDS–PAGE. The amounts of both un-cross-linked monomer and cross-linked oligomers were quantified from the analysis of the protein bands on these gels.

Solution Interactions of Actin with S1. Strong binding of S1 (3.0 μM) to F-actin (between 1.0 and 5.0 μM) was measured in solutions containing 100 mM NaCl, 3.0 mM MgADP , 1.0 mM DTT, and 10 mM PIPES, pH 7.6, at 23 °C. Mixtures of S1 and F-actin were centrifuged in a Beckman Airfuge at 140000g for 15 min. The amounts of S1 bound to F-actin were determined by measuring the concentrations of free, unbound S1 remaining in the supernatant of the centrifuged samples. SDS–PAGE of these samples confirmed that more than 95% of F-actin was pelleted under these conditions. Determinations of actoS1 ATPase activities using the un-cross-linked and cross-linked actins, and of the K_m and V_{max} values for these ATPase activities, followed the protocol described earlier (13).

Stopped-Flow Measurements. The stopped-flow experiments were carried out in an Applied Photophysics SX-18MV (Leatherhead, U.K.) instrument equipped with both excitation and emission monochromators. All measurements were made in solutions containing 25 mM KCl, 2.0 mM MgCl_2 , and 25 mM MOPS buffer, pH 7.4. For light scattering

measurements, both monochromators were set at 380 nm. Temperature was controlled by water (from a refrigerating bath) circulating around the drive syringes and the observation chamber. For each experiment, the data shown are the average of five or six consecutive pushes of stopped-flow syringes. Each experiment was repeated between 3 and 5 times. The data were fitted with a nonlinear least-squares procedure to a single or a double exponential expression from which the rate constants were calculated.

In Vitro Motility Assays. In vitro motility assays were performed at 25 °C as described previously (13, 24). The composition of the assay solution was 25 mM MOPS, pH 7.4, 25 mM KCl, 2.0 mM MgCl₂, 2.0 mM EGTA, 1.0 mM ATP and the glucose-oxidase-catalase system to slow photobleaching of rhodamine phalloidin. Uniformly moving filaments are defined as those with an SD of less than 0.3 × the mean speed (24). Relative force determinations were based on measurements of actin's motion in the presence of external load due to pPDM-labeled HMM. pPDM-HMM, which was prepared as described by Warshaw et al. (25), was mixed at different concentrations with 300 μg/mL HMM prior to their adsorption to coverslips to generate external load in the motility assays.

RESULTS

Cross-Linking Reaction Considerations. Two previously described cross-links of actin by pPDM (18, 19), between Cys-374 and Lys-191 on adjacent protomers on opposite strands, and by ABP, between Gln-41 and Lys-113 on adjacent protomers within the same strand (17), provided us with the means to further probe the structural basis for the inhibition of actin's in vitro motility by its cross-linking with ANP, between Gln-41 and Cys-374 (13). The first reaction, with pPDM, reaches in our hands a limit when about 40–60% of F-actin protomers are cross-linked. This cross-linking limitation was observed by Knight and Offer (18) and ascribed to a competing hydrolysis of the second maleimide moiety in pPDM that is attached to Cys-374. Because of this limitation, we compared in this study the properties of filaments cross-linked by pPDM, ANP, and ABP to ~50% level. In the case of the previously studied ANP cross-linked actin, such cross-linking extent was optimal for reliable measurements of relative forces and filament speeds in the in vitro motility assays. These filaments (~50% cross-linked) moved at ~35% slower speeds and generated ~25% less force with HMM than the un-cross-linked actin, while showing little change in S1 binding and the actoS1 ATPase (13).

The location of the ANP, ABP, and pPDM cross-links on F-actin is shown in Figure 1. In the Holmes model of F-actin structure, the maximum distances between the α-carbons of Gln-41 and Cys-374, Gln-41 and Lys-113, and Cys-374 and Lys-191 are 11.5, 22.3, and 21.4 Å, respectively. The three reagents have similar mean cross-linking spans, between 10.5 and 12 Å. Not surprisingly, given the match of distances and reagent sizes, and the local flexibility of Gln-41 and Cys-374 sites, the ANP and pPDM reactions do not introduce significant distortions in F-actin structure. For the ANP cross-linking, this is deduced from prior EM observations (13), and the recent analysis of Cys-41–Cys-374 disulfide cross-linked yeast mutant actin filaments (16). Moreover, as shown

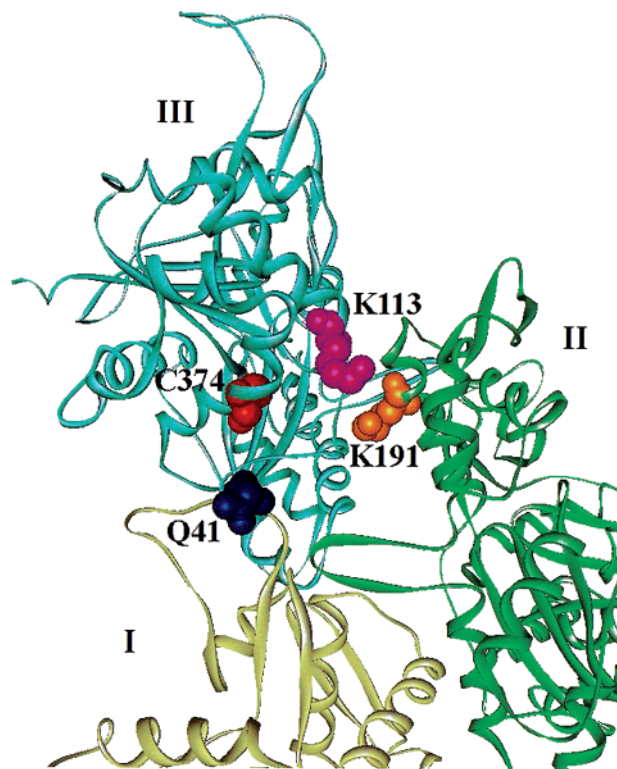


FIGURE 1: Three protomers from the F-actin model of Holmes et al. (15) showing the cross-linked residues. Gln-41 (blue) on protomer I (light green) and Cys-374 (red) on protomer III (blue) are intrastrand cross-linked by ANP. Gln-41 on protomer I and Lys-113 (purple) on protomer III are intrastrand cross-linked by ABP. Cys-374 on protomer III and Lys-191 (orange) on protomer II (dark green) are interstrand cross-linked by pPDM. Protomers I and II are truncated for a better visualization of the cross-linked sites. To this end, actin protomers shown here are also rotated relative to their standard orientation in the Holmes et al. (15) model.

for illustration purposes in Table 1, ANP cross-linking of Gln-41 to Cys-374 yields a concentration distribution of oligomers that corresponds precisely to that predicted for a random probability of cross-linking within F-actin. For F-actin (18), and for other polymers (26), the fraction of protomers, $F_{(n)}$, present in any randomly cross-linked n -mer is given by eq 1:

$$F_{(n)} = n(1 - p)^2 p^{n-1} \quad (1)$$

where n is the number of protomers in the cross-linked oligomer and p is the probability of cross-linking two protomers. The randomness of ANP cross-linking of F-actin (Table 1) shows that successive reactions are independent of each other, which is consistent with little, if any, change in the filament structure.

Similar conclusion was reached before regarding the pPDM cross-linking of F-actin (18), and is confirmed in this study (Table 1). The concentration distribution of pPDM cross-linked oligomers matches also very closely the random cross-linking distribution (with $0.25 \leq p \leq 0.30$ and as illustrated for $p = 0.27$ in Table 1), consistent with minimal, if any, filament structure perturbation by this cross-linking. This is not the case, however, for the ABP (Gln-41–Lys-113) cross-linked actin. Oligomer distribution in this reaction deviates from that predicted by a random process (Table 1, $p = 0.23$), but can be modeled by positively cooperative

Table 1: Observed and Calculated Percentage Distributions of Cross-Linked n -mers in F-Actin^a

n -mer	ANP obsd	pPDM obsd	calcd $p = 0.27$	ABP		
				obsd	$p = 0.23$	$p_1 = 0.23$ $p_{i>1} = 0.41$
1	52.1	53.0	53.3	60.0	59.3	59.3
2	27.4	27.7	28.8 (14.6)	15.5	27.0	16.0
3	11.0	10.7	11.6 (10.5)	10.1	9.4	9.9
4	4.2	3.7	4.2 (6.7)	5.9	2.9	5.4
5	1.2	1.2	1.4 (4.0)	2.9	0.8	2.8

^a The observed percentage distributions of un-cross-linked ($n = 1$) and cross-linked ($n > 1$) actin protomers were obtained from SDS-PAGE analysis of F-actin cross-linked with ANP, pPDM, and ABP. The probability of random cross-linking (p) was obtained using eq 1 [$F_{(1)} = (1 - p)^2$] from the observed fraction of un-cross-linked monomers, where $F_{(1)}$ is the fraction present in the cross-linked filaments. This fraction was determined from the ratio of actin monomer bands in the cross-linked and un-cross-linked samples on SDS gels. (For ANP and pPDM actin, these fractions, 0.521 and 0.530 in row 1, yield p values of 0.278 and 0.272, respectively.) Good fits to the similar experimental distributions of ANP and pPDM cross-linked protomers shown above were obtained with the random reaction model and cross-linking probability $0.25 \leq p \leq 0.30$. For illustration purposes, we show the fit of the distribution calculated for $p = 0.27$. The numbers in parentheses correspond to a reaction model with a positive cooperativity of cross-linking ($p_1 = 0.27$; $p_{i>1} = 0.48$), similar to the model that provides the best fit for the distribution of the ABP cross-linked protomers. For ABP cross-linked actin (containing 60% un-cross-linked monomers), the cross-linking probability $p = 0.23$ was estimated in the same manner as above, from the observed fraction of un-cross-linked monomers. The best fit to the observed distribution of cross-linked protomers ($n > 1$) was obtained with a positive cooperativity cross-linking model and $p_1 = 0.23$ and $p_{i>1} = 0.41$. The random reaction model ($p = 0.23$, no cooperativity) does not fit the experimental data.

cross-linking, with probabilities of $p_1 = 0.23$ and $p_{i>1} = 0.41$ (Table 1). In such a model, the fraction of monomers is, as above, $F_{(1)} = (1 - p_1)^2$, and the fraction of other oligomers ($n \geq 2$) is given by $F_{(n \geq 2)} = n(1 - p_1)^2 \cdot p_1 \cdot p_{i>1}^{n-2}$. Clearly, in this case the initial cross-linking (dimer formation) increases the probability of subsequent reaction steps, indicating at least some changes in F-actin structure. Similar modeled differences between p_1 and $p_{i>1}$ cannot be imposed on the pPDM cross-linking of F-actin since this would lead to a considerable discrepancy between the calculated and experimental distributions of the cross-linked oligomers (Table 1).

Relative Force Measurements. The ability of cross-linked actin to generate force with HMM, relative to that of un-cross-linked actin, was measured by monitoring their in vitro motility against an external load. In these experiments, pPDM-modified HMM (up to 350 $\mu\text{g}/\text{mL}$), which binds actin weakly but is catalytically inactive, was mixed at different concentrations with the unmodified HMM (300 $\mu\text{g}/\text{mL}$) and adsorbed to the coverslips to produce the load. The sliding speeds of actin filaments decreased linearly with an increase in the concentration of pPDM-HMM in the adsorbed solution. As in previous studies (13, 24, 25, 27), the amount of load producing pPDM-HMM needed to arrest actin movement over unmodified HMM was taken as a measure of the force generated with the unmodified HMM.

In the results shown in Figure 2 the speeds of actin filaments were measured for pPDM, ABP, and ANP actin preparations containing 55, 60, and 58% cross-linked protomers, respectively. The speeds of all filaments decrease linearly with an increase in the concentration of the pPDM-

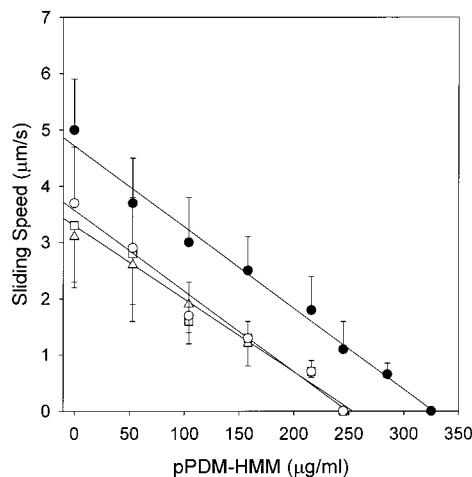


FIGURE 2: Effect of F-actin cross-linking on the relative force produced with HMM as measured by the pPDM-HMM load. Mean sliding speeds of actin filaments were measured as the function of the concentration of pPDM-HMM applied to the assay surface. (●) Un-cross-linked actin; (○) 55% cross-linked pPDM actin; (□) 58% cross-linked ANP actin; and (△) 60% cross-linked ABP actin. The sliding of between 200 and 300 filaments was monitored in each case.

HMM that was mixed with unmodified HMM (300 $\mu\text{g}/\text{mL}$) prior to their adsorption to the coverslips. Straight lines were fitted to the three cross-linked actins, yielding virtually the same extrapolated value of $250 \pm 30 \mu\text{g}$ of pPDM-HMM at which actin motion stops (Figure 2). Higher concentrations of pPDM-HMM ($330 \pm 35 \mu\text{g}/\text{mL}$) were required to stop the motion of un-cross-linked actin filaments (Figure 2). It can be concluded from the ratio of the extrapolated pPDM-HMM concentrations that the three cross-linked actins are indistinguishable in this assay and generate with HMM $\sim 75\%$ of the force produced with the un-cross-linked actin.

In Vitro Motility of Cross-Linked Actins. In the absence of an external load, the mean speeds of the actin filaments compared in Figure 2, i.e., un-cross-linked and pPDM, ABP, and ANP cross-linked, were 5.0, 3.7, 3.3, and 3.1 $\mu\text{m}/\text{s}$, respectively. Thus, with between 55 (for pPDM actin) and 60% (for ABP actin) protomers cross-linked, these filaments move at between 26 and 38% slower speeds than un-cross-linked actin showing a similar impediment to their motion. These data are also included in Figure 3, along with the mean speeds of filaments cross-linked to different extents by ANP and ABP and by a combination of ABP and pPDM reagents.

For ANP F-actin, the maximum extent of cross-linking ($\sim 85\%$ of the protomers) was limited not by the reaction conditions but by the quenching of rhodamine phalloidin fluorescence by ANP. This quenching made it difficult to measure the in vitro motilities of actin filaments containing less than $\sim 15\%$ protomers un-cross-linked by ANP (i.e., containing $\sim 10\%$ actin unlabeled by ANP; see Materials and Methods). The limitation on ABP cross-linking of F-actin ($\sim 75\%$ of the protomers; Figure 3) appears to be related to a lower photo-cross-linking efficiency of ABP compared to ANP. However, the ABP cross-linked F-actin (with $\sim 40\%$ un-cross-linked protomers) could be re-cross-linked with pPDM, which further inhibited its in vitro motility (Figure 3). Clearly, the effects of the two cross-linking reactions on actin's motion are additive. As mentioned above, cross-linking of actin by pPDM alone could not be extended beyond the 50–60% level.

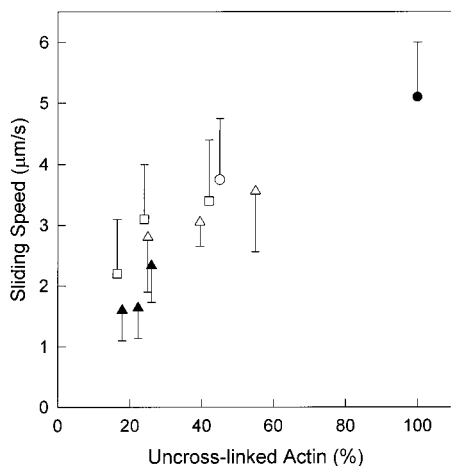


FIGURE 3: Dependence of the sliding speed of actin filaments on the extent of their cross-linking. (●) Un-cross-linked actin; (□) ANP cross-linked actin; (○) pPDM cross-linked actin; (△) ABP cross-linked actin; (▲) 60% cross-linked ABP actin re-cross-linked with pPDM. Mean speeds of sliding filaments are shown as a function of un-cross-linked protomers present in these preparations. (The percentage of un-cross-linked protomers was determined by SDS-PAGE.)

The *in vitro* motilities of the different cross-linked filaments show a similar trend—an increasing inhibition of motion with increasing degree of cross-linking (Figure 3). With such reactions reaching 85% (for ANP) or 83% (for ABP-pPDM) levels of protomer cross-linking, the mean speeds of these filaments are decreased by between 50 and 70% relative to un-cross-linked actin (Figure 3). The overall pattern of motion inhibition as a function of actin cross-linking by the three reagents is similar to that observed before for ANP alone (13), and does not reveal significant differences in the impact of the three cross-linkings on actin's motility. Also, as before (13), deletion of methylcellulose from the assay had no effect on the sliding speeds of the un-cross-linked and cross-linked filaments (at 50 mM ionic strength).

ActoS1 ATPase and S1 Binding. We have shown in a previous study (13) that the binding constant of S1 to actin is not affected by ANP cross-linking of ~50% (and up to ~90%) of its protomers, and that only small changes in the V_{\max} of actoS1 ATPase are caused by such a treatment. Similarly, the cross-linking of actin by pPDM was reported before to have little effect on the myosin binding and the V_{\max} and K_m parameters of actoS1 ATPase (9, 28). We confirmed this observation and compared the S1 binding and actoS1 ATPase properties of F-actin containing 47% and 40% protomers cross-linked by pPDM and ABP, respectively. The ATPase data for the un-cross-linked and cross-linked filaments are visually indistinguishable (Figure 4), and the V_{\max} and K_m values corresponding to them are virtually the same (Table 2). Based on previous studies (13, 24), the unchanged K_m values (compared to un-cross-linked actin) and the absence of a methylcellulose effect on filament sliding reveal that the cross-linking reactions do not decrease significantly the weak binding of S1 to actin. Similarly, the strong binding affinities of S1 for actin in the presence of MgADP showed only small decrease, if any, due to partial cross-linking of F-actin by ABP and pPDM. The K_d values determined for S1·ADP binding to un-cross-linked and cross-

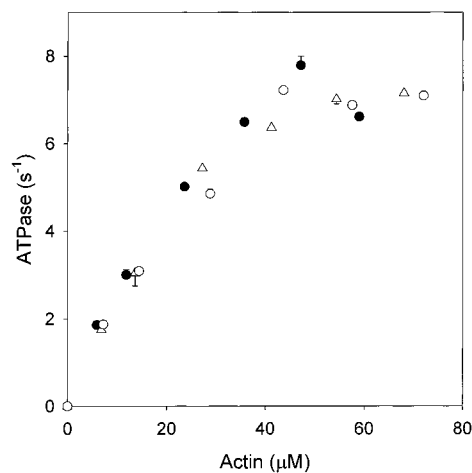


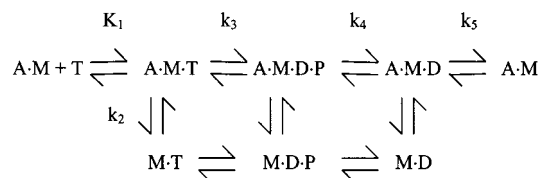
FIGURE 4: ActoS1 ATPase activity of un-cross-linked and cross-linked actin. (●) Un-cross-linked actin; (○) 47% cross-linked pPDM actin; and (△) 40% cross-linked ABP actin. The ATPase turnover rates (micromoles of P_i per micromole of S1 per second) were measured at 25 °C in solutions containing 0.3 μ M S1, variable concentrations of actin, 3.0 mM ATP, 3.0 mM $MgCl_2$, 10 mM KCl, 10 mM imidazole, pH 7.0.

Table 2: S1 Binding and ActoS1 ATPase of Cross-Linked and Un-Cross-Linked Actin^a

F-actin	S1 binding K_d (μ M)	actoS1 ATPase	
		V_{\max} (s^{-1})	K_m (μ M)
un-cross-linked	1.2 ± 0.2	11.0 ± 1.2	27.7 ± 7.4
pPDM cross-linked (47%)	1.7 ± 0.3	10.9 ± 1.0	33.0 ± 7.5
ABP cross-linked (40%)	1.4 ± 0.2	10.8 ± 0.6	30.7 ± 4.2

^a S1 binding to F-actin was measured in the presence of 3.0 mM MgADP (strong binding conditions) as described under Materials and Methods. 47% and 40% of actin protomers were cross-linked in the pPDM and ABP actins, respectively. The V_{\max} and K_m values for actoS1 ATPases provide the best fit for data shown in Figure 4.

Scheme 1



linked F-actin ranged between 1.2 and $1.7 \pm 0.3 \mu$ M (Table 2).

ADP Dissociation from $A \cdot M \cdot ADP$ and $A \cdot M$ Dissociation by ATP. Although the above results, and those on ANP cross-linked actin (13), did not reveal any obvious cause for the inhibition of the mechanical performance (force and sliding speeds) of the cross-linked actin, they did not exclude the possibility that pertinent rate constants in the cross-bridge cycle might be altered by such modifications. Of particular interest are the rates of ADP (D) dissociation from $A \cdot M \cdot ADP$ (k_5 in Scheme 1) and of the subsequent dissociation of $A \cdot M$ by ATP (T) (steps 1 and 2 in Scheme 1).

Changes in the rates of these steps in the cross-bridge cycle could influence the speed and force of the actomyosin motor (29). Because ANP, pPDM, and ABP cross-linked actins showed similar functional properties, but the ANP reaction is the only one that yields preparations with ~90% of the protomers cross-linked (which should improve the detection of possible rate differences), the stopped-flow measurements

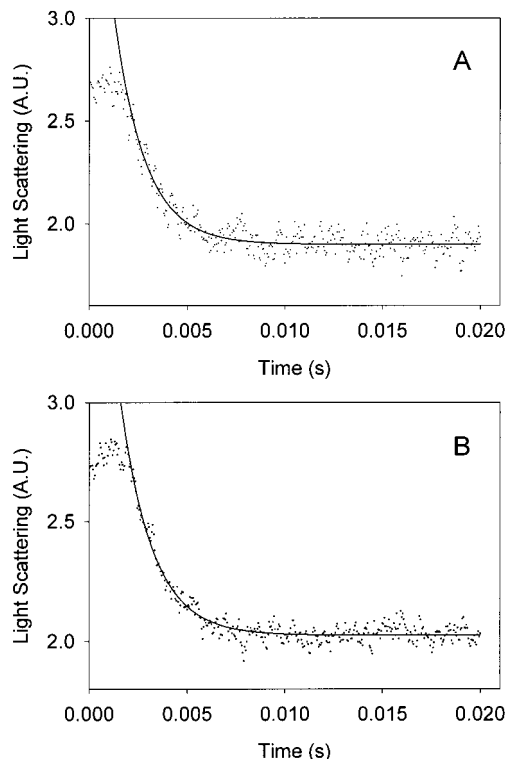


FIGURE 5: Stopped-flow light scattering records of the displacement of mantADP from the actoS1·mantADP ternary complex. (A) Un-cross-linked actin. One syringe contained 5.0 μM actoS1 and 100 μM mantADP, and the other syringe contained 5.0 mM MgATP. (B) As in (A), except that 90% cross-linked ANP actin was used in the complex with S1. Each trace is an average of five repeats of the same experiment. All measurements were done at 5 $^{\circ}\text{C}$. The values of k_{obs} are 634 ± 31 and $618 \pm 26 \text{ s}^{-1}$ for the un-cross-linked (A) and cross-linked (B) actin complexes with S1·mantADP, respectively. The solid lines are the best fits to single exponentials.

of the above rates were carried out on such a highly cross-linked ANP-actin.

The rate of ADP dissociation from actoS1 (k_5 in Scheme 1) can be determined by measuring (by light scattering) the limiting rate of ATP-induced dissociation of S1 from actin at high ATP concentrations (30). Because the rates of ADP dissociation from both actoS1 and ANP cross-linked actoS1 were too fast ($\sim 1000 \text{ s}^{-1}$ at 5 $^{\circ}\text{C}$) for reliable comparisons, we employed mantADP instead of ADP in these observations (31). Figure 5 shows that mixing 5.0 mM ATP with actoS1·mantADP and ANP cross-linked actoS1·mantADP leads to actoS1 dissociation at the observed rates of 634 ± 31 and $618 \pm 26 \text{ s}^{-1}$, respectively. The same rates were observed also upon mixing the actoS1·mantADP complex with 10 mM ATP, indicating that these are the limiting rates. These results reveal that the rate of ADP dissociation from actoS1 is not changed by extensive ($\sim 90\%$) ANP cross-linking of actin.

The ATP-induced dissociation of cross-linked and un-cross-linked actoS1 was monitored at 20 $^{\circ}\text{C}$ by light scattering, after mixing ATP with the complex (Figure 6). The observed rate constants showed virtually identical linear dependence in the range between 10 and 50 μM ATP (Figure 6C), irrespective of actin cross-linking. ATP binding was analyzed according to Scheme 1, in which K_1 defines the rapid binding equilibrium between A·M and ATP and k_2 , the rate constant for actin dissociation from A·M·T, is rate-limited by the isomerization of the ternary A·M·T complex (30). The observed rate constant for ATP-induced dissociation

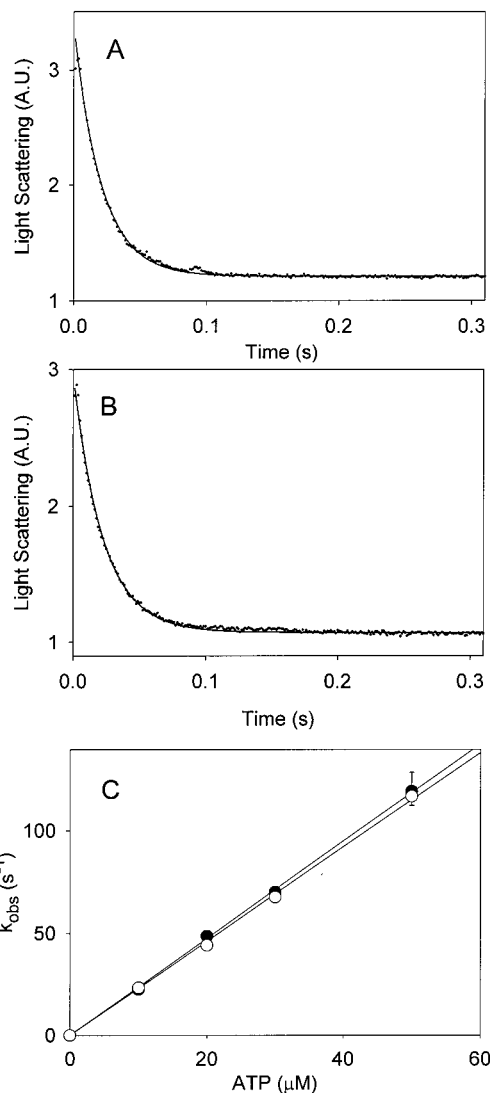


FIGURE 6: ATP-induced dissociation of actoS1. (A) Observed light scattering changes on mixing 4.0 μM actoS1 (syringe 1) with 20 μM ATP (syringe 2); $k_{\text{obs}} = 49.0 \pm 0.3 \text{ s}^{-1}$. (B) As in (A), except that 90% cross-linked ANP actin was used in the complex with S1; $k_{\text{obs}} = 44.5 \pm 0.3 \text{ s}^{-1}$. The solid lines in (A) and (B) are the best fits to single exponentials. All measurements were done at 20 $^{\circ}\text{C}$. (C) The observed rate constants for ATP-induced dissociation of the actoS1 complex formed with cross-linked (\circ) and un-cross-linked (\bullet) actin. The slopes of the best-fit lines define the apparent second-order rate constants (K_1k_2) of $(2.39 \pm 0.03) \times 10^6$ and $(2.32 \pm 0.05) \times 10^6 \text{ M}^{-1} \text{ s}^{-1}$ for the un-cross-linked and cross-linked actin complexes with S1, respectively. The error bars are too small to be seen except at the highest actin concentration.

tion of actin from A·M·T is given by (30)

$$k_{\text{obs}} = K_1k_2[\text{ATP}]/(1 + K_1[\text{ATP}])$$

Assuming that $K_1[\text{ATP}] \ll 1$, then $k_{\text{obs}} = K_1k_2[\text{ATP}]$. The apparent second-order binding constants, K_1k_2 , derived from the slopes in Figure 6C are $(2.32 \pm 0.05) \times 10^6$ and $(2.39 \pm 0.03) \times 10^6 \text{ M}^{-1} \text{ s}^{-1}$ for the ANP cross-linked and un-cross-linked actoS1, respectively. This shows that actin cross-linking by ANP does not impair actoS1 dissociation by ATP and the coupling between the ATP and actin sites on S1.

DISCUSSION

Equivalent Effects of ANP, pPDM, and ABP Cross-Linking on Actin Function. Our previous study on ANP intrastrand

cross-linked actin (between Gln-41 and Cys-374) suggested that immobilization of the subdomain 2/subdomain 1 interprotomer interface uncouples the mechanical function from other aspects of actomyosin interactions (13). For example, in the ~50% cross-linked actin, S1 binding and actoS1 ATPase were little changed, while the in vitro motility and force generated by such filaments were inhibited. The main goal of this study was to test the spatial specificity of the “mechanical inactivation” of actin by the above cross-linking. The observation that intraprotomer cross-linking of Gln-41 to Lys-50 did not cause such an effect indicated that motion and force inhibition in ANP cross-linked actin are related to the immobilization at the interprotomer interface of either the DNase I loop, the C-terminus, or both (14). The previous mapping of pPDM and ABP actin cross-linking to the Cys-374–Lys-191 (19) and Gln-41–Lys-113 (17) pairs, respectively, has provided an attractive opportunity for further structural dissection of the inactivation of the actomyosin motor by actin cross-linking.

As before (13), most of our experiments were carried out with filaments containing between 40 and 60% cross-linked protomers. This choice was made because of reaction limitations (with pPDM and ABP) and the need to achieve sufficient sensitivity in the relative force measurements in the in vitro motility assays. In analogy to ANP cross-linking (13), and in agreement with the previous results on pPDM cross-linked actin (9, 28), neither pPDM nor ABP cross-linkings had any significant effect on the strong S1 binding to actin (in the presence of MgADP) and the V_{\max} and K_m parameters of actoS1 ATPase. Furthermore, extending the analogy to ANP cross-linked actin, the pPDM and ABP cross-linked filaments (~50%) showed similar inhibition of their motion and force generation with HMM. More extensive cross-linking of actin by either ANP or a combination of pPDM and ABP resulted in a greater inhibition of filament motion (Figure 3). These results show that all three cross-linkings, intrastrand Gln-41–Cys-374 and Gln-41–Lys-374 and interstrand Cys-374–Lys-191, cause similar inhibition of force generation without impairing other aspects of actomyosin interactions. The common denominator in these three reactions, involving three different sites, is that in each case a structural component of the subdomain 2/1 interprotomer interface, either the DNase I binding loop or the C-terminus, is cross-linked to another site. This shows that dynamic changes at that interface may be blocked by either one of the three reactions. As suggested before (3), the conformation and the changes at this interprotomer interface may be highly coordinated. It appears that the mechanical output of the actomyosin motor depends on such coordinated changes at the Gln-41 and Cys-374 sites. Either the dynamic flexibility remaining at the un-cross-linked site, when the other one is cross-linked, is inadequate for force generation, or the cross-linking results in a different structural environment for S1.

On the Cross-Linking Inactivation of the Actomyosin Motor. Previous electron microscopy and image reconstruction of ANP cross-linked filaments did not reveal any substantial structural changes due to such a reaction (13). This has been also confirmed for disulfide cross-linked (Cys-41 to Cys-374) yeast actin mutant (16), and is indicated as well by the random nature of the ANP cross-linking of F-actin (Table 1). The ABP cross-linking, unlike the random

pPDM reaction (18) (Table 1), appears to cause some structural perturbations in F-actin as indicated by the positive cooperativity of this reaction.

In principle, filament sliding speeds could be decreased due to slower rates of ADP release from AM·ADP or AM dissociation by ATP (Scheme 1). Such changes would increase the duration of the power stroke, or impede actomyosin detachment, and therefore decrease filament speeds (29). This possibility is not supported by the present results which do not detect differences in the rates of these steps between extensively cross-linked (by ANP) and un-cross-linked F-actin. Moreover, while slower ADP release from AM·ADP would decrease filament speeds, it would also increase force production with HMM, which is contrary to our observations.

If changes in structure and in the kinetic rates of pertinent steps in the cross-bridge cycle are excluded as a possible cause for inhibition of the actomyosin motor, the flux of force-generating cross-bridges through the cycle must be considered next. We showed before that filaments reconstituted from purified cross-linked dimers retained ~50% of their in vitro motility (13). Their force generation may be related primarily to the fraction of actin protomers sharing un-cross-linked subdomain 2/1 interprotomer contacts (all contacts between the cross-linked dimers), or to an average, decreased force generation by all actin protomers in the filaments. The following consideration favors the former possibility. In the random cross-linking model (eq 1), the fraction of un-cross-linked contacts is given by the probability of not cross-linking two adjacent protomers, i.e., is equal to $1 - p$. For F-actin with ~50% of its protomers cross-linked, this corresponds to ~70% un-cross-linked and ~30% cross-linked interprotomer contacts (eq 1). The inhibition of force observed for such ~50% cross-linked filaments (~25% inhibition; Figure 2) fits reasonably well to this model. Thus, we propose that the loss of force-generating actomyosin interactions is tightly coupled to the fraction of interprotomer contacts that are cross-linked. In this model, little, if any, force is generated by HMM with a pair of cross-linked actin protomers, while normal force is developed with un-cross-linked pairs of adjacent protomers in the filament.

Because myosin binding, actoS1 ATPase, and kinetic rates of actoS1 interactions are not changed significantly by actin cross-linking, the proposed loss of ~30% of force-generating actomyosin interactions (in ~50% cross-linked filaments) should not necessarily result in lower filament speeds in the in vitro motility assays. A decrease in HMM density on the coverslips does not reduce significantly filament speeds until a low HMM threshold concentration is reached (13, 29). Thus, in our case, the cross-linked actin pairs that are assumed to produce little (if any) force, but which interact with HMM, probably introduce some load into the system and thus slow the motion of filaments. This behavior is reminiscent of pPDM SH1–SH2 cross-linked HMM, which introduces external load into in vitro motility assays (Figure 2) (when mixed with unmodified HMM) by its weak, but enzymatically and mechanically futile binding to actin. However, the load attributed here to the cross-linked actin must be smaller than that produced by the weakly binding HMM. This is because the motion of un-cross-linked actin is stopped at ~1:1 ratios of pPDM HMM to HMM (Figure 2), while the speed of actin filament with approximately

equal frequency of cross-linked and un-cross-linked actin interprotomer contacts (i.e., $p = 1 - p = 0.5$; 25% of the actin protomers are un-cross-linked) is reduced by between 50 and 60% (Figure 3).

A question may be raised also about the possibility that the reduced flexibility of cross-linked filaments might inhibit their ability to find and attach to the HMM on the coverslip. This scenario is unlikely because of the high density of HMM on the coverslips used in our experiments. Homsher et al. (32) determined under identical experimental conditions that as many 130 ± 11 myosin heads are available per micrometer of actin on the motility surface. Thus, filaments ranging in length between 1 and 15 μm (in our motility assays) can interact with ~ 100 –2000 myosin heads (32). It may be noted also that a decreased flexibility of actin filaments does not necessarily result in a slower sliding over myosin. Tropomyosin, which increases the persistence length (a measure of stiffness) of F-actin from 9 to 21 μM (33), appears to have no effect on filament speeds (32, 34), and under some conditions may even increase their speed (35).

Although suggestive, the above considerations do not prove yet that the cross-linking reactions produce two populations of actin protomer pairs in the filaments—mechanically active and inactive—and do not simply decrease the mean unitary force produced per power stroke across the entire filament, for both the cross-linked and un-cross-linked protomer pairs. Ultimately, optical trap measurements on single filaments will be needed to clarify the nature of the observed force generation inactivation in the cross-linked actin filaments and the possible presence of mechanically active and inactive actin protomers in the filaments. Preliminary experiments of this type appear to support the idea that there are myosin binding sites in the cross-linked filaments that support normal unitary mechanics and kinetics of actomyosin interactions whereas there are other sites that do not support such interactions. (J. Baker and D. M. Warshaw, personal communication). Irrespective of that, our present results show that the uncoupling between actomyosin interactions and force generation is not a unique result of an interprotomer cross-linking between Gln-41 and Cys-374. Our data suggest that in general, cross-linking immobilizations of the subdomain 2/1 interprotomer interface produce similar results and thus strengthen the evidence for the importance of actin filament dynamics to the force generation by actomyosin.

ACKNOWLEDGMENT

We thank Dr. K. Seguro for the gift of bacterial transglutaminase and Dr. A. Bobkov for helpful discussions and assistance with the preparation of the manuscript.

REFERENCES

- McGough, A., Pope, B., Chiu, W., and Weeds, A. (1997) *J. Cell Biol.* 138, 771–781.
- Hanein, D., Matsudaira, P., and DeRosier, D. J. (1997) *J. Cell Biol.* 139, 387–396.
- Owen, C., and DeRosier, D. J. (1993) *J. Cell Biol.* 123, 337–344.
- McGough, A., and Chiu, W. (1999) *J. Mol. Biol.* 291, 513–519.
- Galkin, V. E., Orlova, A., Lukoyanova, N., Wriggers, W., and Egelman, E. H. (2001) *J. Cell Biol.* 153, 75–86.
- Orlova, A., and Egelman, E. H. (1993) *J. Mol. Biol.* 232, 334–341.
- Orlova, A., and Egelman, E. H. (1995) *J. Mol. Biol.* 245, 582–597.
- Egelman, E. H., and Orlova, A. (1995) *Curr. Opin. Struct. Biol.* 5, 172–180.
- Prochniewicz, E., and Yanagida, T. (1990) *J. Mol. Biol.* 216, 761–772.
- Schwytter, D. H., Kron, S. J., Toyoshima, Y. Y., Spudich, J. A., and Reisler, E. (1990) *J. Cell Biol.* 111, 465–470.
- Schwytter, D. H., Phillips, M., and Reisler, E. (1989) *Biochemistry* 28, 5889–5895.
- Hegyi, G., Mak, M., Kim, E., Elsinga, M., Muhrad, A., and Reisler, E. (1998) *Biochemistry* 37, 17784–17792.
- Kim, E., Bobkova, E., Miller, C. J., Orlova, A., Hegyi, G., Egelman, E. H., Muhrad, A., and Reisler, E. (1998) *Biochemistry* 37, 17801–17809.
- Eli-Berchoer, L., Hegyi, G., Patthy, A., Reisler, E., and Muhrad, A. (2000) *J. Muscle Res. Cell Motil.* 21, 405–414.
- Holmes, K. C., Popp, D., Gebhard, W., and Kabsch, W. (1990) *Nature* 347, 44–49.
- Orlova, A. A., Galkin, V. E., VanLoock, M. S., Kim, E., Shvetsov, A., Reisler, E., and Egelman, E. H. (2001) *J. Mol. Biol.* 312, 95–106.
- Hegyi, G., Michel, H., Shabanowitz, J., Hunt, D. F., Chatterjee, N., Healy-Louie, G., and Elzinga, M. (1992) *Protein Sci.* 1, 132–144.
- Knight, P., and Offer, G. (1978) *Biochem. J.* 175, 1023–1032.
- Elzinga, M., and Phelan, J. J. (1984) *Proc. Natl. Acad. Sci. U.S.A.* 81, 6599–6602.
- Spudich, J. A., and Watt, S. (1971) *J. Biol. Chem.* 246, 4866–4871.
- Godfrey, J. E., and Harrington, W. F. (1970) *Biochemistry* 9, 886–893.
- Weeds, A., and Pope, B. (1977) *J. Mol. Biol.* 111, 129–157.
- Margossian, S. S., and Lowey, S. (1982) *Methods Enzymol.* 85, 55–72.
- Miller, C. J., Wong, W. W., Bobkova, E., Rubenstein, P. A., and Reisler, E. (1996) *Biochemistry* 35, 16557–16565.
- Warshaw, D. M., Derosiers, J., Work, S., and Trybus, K. (1990) *J. Cell Biol.* 111, 453–463.
- Tanford, C. (1966) in *Physical Chemistry of Macromolecules*, pp 138–150, Wiley, New York.
- Haeberle, J. R. (1994) *J. Biol. Chem.* 269, 12424–12431.
- Knight, P., and Offer, G. (1980) *Biochemistry* 19, 4682–4687.
- Uyeda, T. Q. P., Kron, S. J., and Spudich, J. A. (1990) *J. Mol. Biol.* 214, 699–710.
- Furch, M., Geeves, M. A., and Manstein, D. J. (1998) *Biochemistry* 37, 6317–6326.
- Woodward, S. K. A., Eccleston, J. F., and Geeves, M. A. (1991) *Biochemistry* 30, 422–430.
- Homsher, E., Lee, D. M., Morris, C., Pavlov, D., and Tobacman, L. S. (2000) *J. Physiol.* 524.1, 233–243.
- Isambert, H., Venier, P., Maggs, A. C., Fattoum, A., Kassab, R., Pantaloni, D., and Carlier, M. F. (1996) *J. Biol. Chem.* 270, 11437–11444.
- VanBuren, P., Palmiter, K. A., and Warshaw, D. A. (1999) *Proc. Natl. Acad. Sci. U.S.A.* 96, 12488–12493.
- Bing, W., Razzaq, A., Sparrow, J., and Marston, S. (1998) *J. Biol. Chem.* 273, 15016–15021.